



HAL
open science

Procedure for Spaced Mesh Modeling from Digital Images: Example of the Leaf Sheath of the Coconut Palm *Cocos Nucifera* L. (2D)

Jimmy Nagau, Lisa Vidil, Cristel Onesippe Potiron, Ketty Bilba, Marie-Ange Arsene, Jean-Luc Henry

► To cite this version:

Jimmy Nagau, Lisa Vidil, Cristel Onesippe Potiron, Ketty Bilba, Marie-Ange Arsene, et al.. Procedure for Spaced Mesh Modeling from Digital Images: Example of the Leaf Sheath of the Coconut Palm *Cocos Nucifera* L. (2D). ACS Omega, inPress, 7 (39), pp.34789-34800. 10.1021/acsomega.2c02748 . hal-04558295

HAL Id: hal-04558295

<https://hal.science/hal-04558295v1>

Submitted on 16 Jul 2024

HAL is a multi-disciplinary open access archive for the deposit and dissemination of scientific research documents, whether they are published or not. The documents may come from teaching and research institutions in France or abroad, or from public or private research centers.

L'archive ouverte pluridisciplinaire **HAL**, est destinée au dépôt et à la diffusion de documents scientifiques de niveau recherche, publiés ou non, émanant des établissements d'enseignement et de recherche français ou étrangers, des laboratoires publics ou privés.

Procedure for Spaced Mesh Modeling from Digital Images: Example of the Leaf Sheath of the Coconut Palm *Cocos Nucifera* L. (2D)

Jimmy Nagau,* Lisa Vidil, Cristel Onesippe Potiron, Ketty Bilba, Marie-Ange Arsene, and Jean-Luc Henry



Cite This: *ACS Omega* 2022, 7, 34789–34800



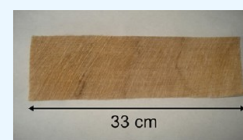
Read Online

ACCESS |

Metrics & More

Article Recommendations

ABSTRACT: The characterization of the two-dimensional (2D) leaf sheath of the coconut palm *Cocos nucifera* from digital images is part of a research project that focuses on the feasibility of using a local natural resource, the leaf sheath of the coconut palm *C. nucifera* (2D), for the development of a green composite material and the analysis of the influence of this type of reinforcement, which has the advantage of being naturally woven, on the properties of the biocomposites obtained. In order to characterize these properties, it is essential to extract information from the leaf sheath samples. This work consists of counting and evaluating the thicknesses and directions of all the fibers that make up the sheath. In simple cases, from sample photographs, we wish to propose a processing chain capable of automating this extraction process. We are interested here only in samples with areas of spacing between the fibers. Therefore, our proposal cannot be a solution for tightly packed fibers. The data are represented by photographs of leaf sheath samples taken with a high-resolution microscope. This results in color images of 3000 × 3000 pixels. In the following, we will call EI a space in which it is possible to locate a pixel by its spatial coordinates, and we will call EC another space in which it is possible to locate the color of a pixel by its colorimetric coordinates. In EI, the set representing the pixels denoting the fiber will be denoted EF and that representing the void areas will be denoted EV. From these starting sets, the work consisted of finding a process that allows the extraction and characterization of points of interest representing the leaf sheath.



INTRODUCTION

Integration of local natural resources, such as the two-dimensional (2D) leaf sheath of the coconut tree *Cocos nucifera* L., in the design and development of green materials is an important issue.¹ Indeed, this reinforcement is naturally woven. In this context, the innovation consists of replacing the petrochemical or organic compounds generally used in the construction sector by vegetable material, for green composite elaboration. In order to propose the leaf sheath tissue as part of construction product as well as synthetic fibers of known and regular morphology, a large number of samples of these fabrics have to be evaluated in terms of morphological, structural, and mechanical properties. The work is carried out on the basis of images obtained by optical microscopy. The images will be exploited in algorithms in order to provide, in the case of low-complexity woven support (loose mesh), a large volume of primitives that can be used in pattern analysis or statistical studies. During the investigations, we are positioned at the level of image processing of the leaf sheath of the coconut palm *C. nucifera* L. (2D), in order to extract primitives automatically using dedicated algorithms. First, we will propose a study of the acquired images; then, we will present two algorithms whose goal is to extract and to characterize the leaf sheath tissue fibers. These algorithms have been tested with experimental and simulated data but also with real data from different leaf sheath samples. Obtained results are encouraging because they allow the extraction of first characterization data.

CONTEXT AND ISSUES

Context of Study. The aim of the work was to study the potentiality of leaf sheaths of coconut tree to make naturally woven composites. Indeed, it is a vegetable sustainable material abundantly available in Guadeloupe. Moreover, this unexploited resource is a woven material, a natural textile, which does not need manufacturing to present a textile form.

Quantitative and qualitative morphological characterizations of fibers and modeling of textile meshing are elements of great importance in the field of eco-materials.^{2,3} Faced with the challenges of sustainable development in recent decades, the potential use of plant fibers as reinforcement in composite materials has been the subject of research.^{4,5} Most of these studies concern organic matrices reinforced by short natural fibers, usually randomly distributed in the matrix.^{6,7}

Prior to the development of biocomposites, an exploratory approach of the leaf sheath fibers needs to be led in order to characterize and to model their fibers because the proper use of the composites depends on the properties of the latter. Hence, evaluation of morphological properties, which partly deter-

Received: May 3, 2022

Accepted: September 7, 2022

Published: September 22, 2022



mines physical and mechanical properties of fibers^{8,9} and those of the composites, is necessary.

The use of professional software and the increasing computational power of modern computer systems make it possible to efficiently solve computational problems concerning the deformation of woven structures. However, in order to obtain accurate results with this approach, an adequate description of the geometry of the weaving of the threads in the woven structure is necessary.¹⁰ Consequently, this image analysis was carried out in order to provide geometrical parameters of the leaf sheaths according to its future applications, to rationalize its organization, and to model this organization by developing a digital image analysis application.

Problematics. Characterization of the leaf sheath of the coconut palm *C. nucifera* L. (2D), based on digital images (see Figure 1), is a part of the study of the feasibility of the use of

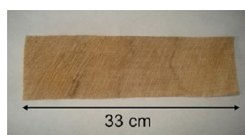


Figure 1. Image of a coconut leaf sheath *Cocos nucifera* L. (2D).

this local natural and woven resource as reinforcement of biocomposites. It is essential to extract numerical information from leaf sheath samples; treatment carried out consists of counting the number of fibers per leaf sheath and evaluating their thickness and direction using a digital image. In cases that do not present a high level of complexity, our goal is to propose a processing chain capable of automating this extraction process.

We are only interested here in samples showing fiber spacing zones. Therefore, our proposal cannot be a solution in the case of tight fibers with no empty spaces. The data are represented by photographs of leaf sheath samples taken with a binocular magnifier. This results in color images with a size of 3000 × 3000 pixels as shown in Figure 2.

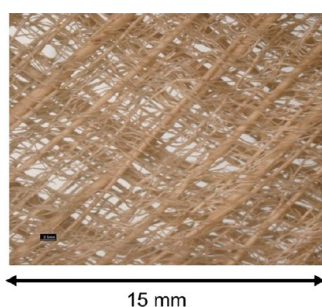


Figure 2. Sample of *Cocos nucifera* L. coconut leaf sheath mesh (2D).

The previous image is split into subsets as shown in Figure 3 to allow parallel processing of the operations.

In the following, we note by EI the space in which it is possible to locate a pixel by its spatial coordinates and by EC that in which the detection of the color of a pixel is made, thanks to its colorimetric coordinates. In EI, the set representing the pixels designating the fiber will be denoted as EF and that representing the empty areas will be denoted as EV. From these starting sets, the work consists of finding a

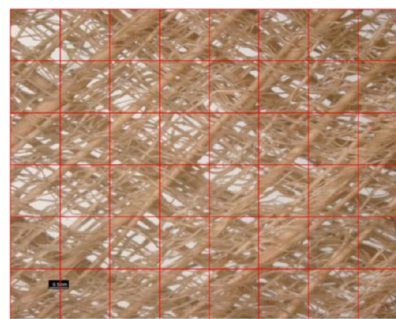


Figure 3. Representation of the grid used in the design of sub-images for algorithmic treatments (each red square measures 1.875 mm on a side).

process that allows the extraction and characterization of interesting points representing the leaf sheath.

State of Art. In the literature, the morphological characteristics of the fibers and/or fibrous cells composing them mainly concern their length, thickness, or cross-sectional area as well as the shape of their cross section and the topography of their surface.^{2,3} The evaluation of quantitative parameters can be carried out directly on fibrous samples when their size allows it. In this case, measuring instruments are used.

1. Fiore et al. evaluate the length of *Arundo* fibers after mechanical extraction using a ruler graduated in centimeters and millimeters.¹¹
2. It is the same for assessing the length of flax, yucca, and Nile rose fibers,^{12–14} respectively.
3. In addition, in other research, caliper^{15–17} and micrometer^{18–20} have been used to measure the diameter of the fibers under study.
4. To evaluate these morphological characteristics, other authors have used non-contact techniques using optical instruments (binocular magnifier, optical microscope, and scanning electron microscope) to acquire images of the samples and image processing software (Image J, Motic Images, ArchiMed, and Leica) with which distance measurements are determined between two points positioned by the operator, and the areas are calculated for the surface delimited by the user.^{8,21–26}

The assessment of qualitative morphological parameters such as the cross-sectional shape of the fibers and/or fibrous cells and the topography of their surface is made by observing images taken by optical instruments. Indeed, from electron microscope images, Amel et al. observed the impact of different extraction methods on the cross-sectional shape and surface configuration of kenaf fibers.²⁷ The observations by optical microscopy of raw gomuti fibers²⁸ reveal observations under an optical microscope, that they have a transverse ellipsoidal or circular shape and a surface covered with cavities containing white substances, the thyllas.

In order to pursue studies in the field of eco-materials reinforced by short natural fibers, research projects in the recent years have been carried out on the extension of the use of biocomposites by developing vegetable textile reinforcements.^{6,29} Compared to materials reinforced by randomly distributed short fibers, textile composites have better mechanical properties in the direction of fiber reinforcement^{30,31} and therefore are able to be used in high stress applications.^{6,32} Vegetable textile reinforcements consist of the

entanglement of several yarns that are made up of the assembly of thousands of lignocellulosic fibers. Three main architectures of textile exist: (1) woven, (2) braided, and (3) knitted,^{33,34} whose several variants for each mode of interweaving is the origin of the plurality of textile structures that can be developed. Faced with this observation, in order to anticipate and to optimize the development of textile preforms, many studies on the prediction of their mechanical properties and their composites have emerged. Indeed, although experimental mechanical tests are direct and efficient, they are often long, difficult to implement, expensive, and destructive.^{35,36} Models for simulating the mechanical behavior of textile reinforcements first require the most accurate textile mesh modeling possible,^{37,38} which usually appeals as input parameters, the shape and geometric dimensions of the yarn cross section, the distance between yarns, the yarn crossing pattern, and the number of yarns in each direction.^{39,40} These latter elements are to be filled in by the user. On this principle, many authors have developed geometric reconstruction models of the structure of textiles in two dimension and/or three dimension in order to predict their mechanical behaviors. For example, the WiseTex software was developed by Lomov et al.^{41–43} and Verpoest and Lomov,⁴⁴ from which the Gentex model developed by Couegnat⁴⁵ was derived. Sherburn of the University of Nottingham developed the TexGen software during his PhD thesis.⁴⁶ Commercial software packages with comparable functionality include TechText CAD and Weave Engineer, developed by TexEng Softawre Ltd.⁴⁷ Based on the same basic principle of previous programs, Hivet and Boisse proposed a geometric model of woven structures.^{48,49} A significant contribution for 3D woven fabrics has been made to this model.^{50,51}

Thus, it appears, at the end of this state of the art, that the methods of appreciation and evaluation of the qualitative and quantitative morphological characteristics of fibers, found in the literature, require the intervention of the operator. Moreover, textile reconstruction models require as input data the geometrical and structural properties of the representative elementary volume, which constitutes the smallest elementary cell, allowing, by repetition, to reconstruct the entire textile.^{39,42} Indeed, man made textiles form quasi-uniform periodic environments. Thus, these models cannot be transposed to reinforcements naturally in textile form, such as the leaf sheaths of the coconut tree *C. nucifera* L., their natural character, their maturity, and the different pedoclimatic conditions of coconut tree growth, conferring a great variability in the qualitative and quantitative characteristics defining their architecture.⁵² In view of these observations, this study is part of a contribution to the characterization of coconut leaf sheath fibers and to the 2D modeling of their mesh using digital image-processing methods, freeing itself from any operator intervention, thus saving time. This work consists, on the one hand, of the exploratory phase, of automating the extraction of morphological characteristics of the fibers, namely, their thickness and their orientation with respect to the horizontal, and on the other hand, of the reconstruction in 2D of the fibrous organization of the coconut leaf sheaths that will help the user to rationalize the complex architecture of the leaf sheaths as well as allow the development of models for the mechanical simulation of leaf sheaths in a second step.

MATERIALS AND METHODS

We have two types of data at our disposal in this work,

- 5 Real data that are represented by images obtained with the binocular loupe. The latter consists of a Nikon 1000 camera, whose lens is equipped with a Nikon DXM 1200F digital camera. The software implemented in this system allows the acquisition of images that are 3000 pixels wide by 3000 pixels high within the framework of our use. These images are cut into thumbnails in the algorithmic treatments that we have implemented.
- 6 Simulated data generated by Algorithm 3, which allows us to provide for each randomly generated fibers, their positions, directions, and thicknesses.

As part of the evaluation of the algorithms implemented for the reconstruction and characterization of the fibers,

- 7 Concerning the position of the fibers in space, we use the sensitivity and specificity parameters for the validation of the fiber representation. These parameters are standard criteria used in image processing in order to validate the good representation of the results provided by the algorithms.
- 8 Concerning the thicknesses and directions provided by the algorithms,
 - For real data, we use the image J software for comparison and student tests in statistics.
 - For simulated data, we automatically compare the simulated data with the data provided by the algorithms.

DATA AND SOFTWARE AVAILABILITY

In this analysis, we had 5 images from the scanning electron microscope of dimensions 3840 × 3072. Each of these images generated 42 images of dimension 500 × 500 for a total of 210 real data. In this study, we have generated simulated images for the evaluation of the proposed algorithms. For these images, we varied the number of fibers and their representation. In this context, we have a total of 480 simulated data. All these images in the analysis context are independent, as we evaluate the local properties of each of the fibers.

The processing chain starts from a sub-image taken with an electron microscope; a set of algorithms is linked to this data in order to provide for each of the coordinates designating a portion of fiber: the thickness and the direction.

The first phase is devoted to the pre-processing of the image. This part is not presented in the book. It represents 5 treatments that work in order: cutting the image into thumbnails to reduce the processing time by reducing the exploration area; a segmentation method (MeanShift) to obtain a reduction of the colorimetric diversity (fiber and background); detection of the points representing the edges of the fibers; places of passage of the color of the fibers to the background color; and a fusion of the remaining similar colors to obtain two colors by classification.

The second phase allows the extraction of the desired knowledge from three algorithms which constitute our contribution. We in order: an algorithm that provides a definition of the contours of each of the void spaces in a fiber image—we use the Freeman coding on the result of the detector of contours and then we cut it into segments whose orientation and size are based on a principal component analysis; an algorithm that performs the mapping of the walls

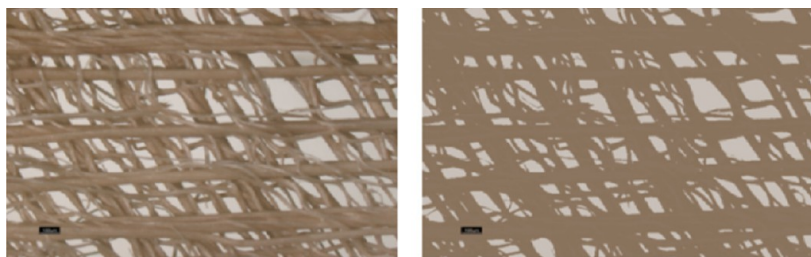


Figure 4. Illustration of the segmentation process on a leaf sheath sample. On the left, an original image; on the right, its segmented result.

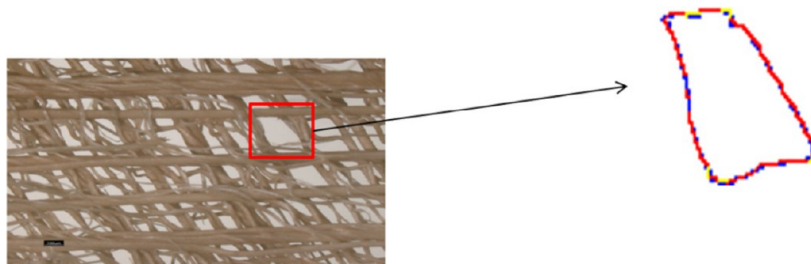


Figure 5. Construction of an edge. On the left, sample of coconut leaf sheath made of woven fibers; on the right, decomposition of the empty area edge into fitting segments. In blue are designated the contours of a void area. In red are represented chains of mini segments of similar direction. In yellow are represented sequences of mini segments whose directions are not similar.

of the empty spaces—these walls delimit portions of fibers; and an algorithm that allows the construction of close to the completeness of the fibers from their portions initially extracted.

■ PROCESS OF SEARCHING FOR THE POINTS OF A FIBER IMAGE DESIGNATING THE LEAF SHEATH

In the first step, we divide the pixels of the image into two groups by performing a segmentation. The purpose of this operation is to extract the pixels designating the leaf sheath that we store in the EF set, while the pixels designating empty spaces are stored in EV. We use for this purpose the colorimetric space EC, because for this type of representation, the difference between the colors of the fiber and the empty spaces is rather marked. We place in EC two class centers resulting from a study of the average observed color of the fibers, for the first one, and of the empty spaces, for the second one. The segmentation process on a leaf sheath sample is carried out by expression 1; its result is shown in Figure 4.

$$\forall P_{(x,y)} \begin{cases} \text{color}(P_{(x,y)}) & \text{if } d(\text{color}(P_{(x,y)}), \text{CMF}) \\ = \text{CMF} & < d(\text{color}(P_{(x,y)}), \text{CMV}) \\ \text{color}(P_{(x,y)}) & \text{else} \\ = \text{CMV} & \end{cases} \quad (1)$$

where $P_{(x,y)}$ is the x and y coordinates of a pixel, CMF is the average color designating the fiber, CMV is the average color designating the empty areas, $\text{color}()$ is the function providing color, and $d()$ is the function providing the Euclidean distance.

The second computational step in the search for the points of a fiber image is dedicated to the creation of a new set named EFF. Its role is to represent the set of pixels of the image designating the edges of the fiber, which is described using expression 2.

$$\text{EFF} = \{P_{(x,y)} \mid \forall \lambda > 0 \Rightarrow B(P_{(x,y)}, \lambda) \cap \text{EF} \neq \emptyset \text{ and } B(P_{(x,y)}, \lambda) \cap \text{EV} \neq \emptyset\} \quad (2)$$

where $B(P_{(x,y)}, \lambda)$ is a ball of center $P(x, y)$ and radius λ .

At the end of the treatment, in order to identify only the areas of net fibers, we introduce a last set noted C. It comes from the result of a contour detector, designating the pixels of the image placed on areas of strong variation in EC. Using all these tools and from EV space, we represent each contour of the related pixel groups using a set of fitting segments.

Edge Segmentation of Empty Areas. In the set of EV, we perform a first construction of the edge for related pixels groups. We call T_i the set of labeled related pixels i in EV and F_i the set of pixels that bound its boundary. We then represent each set F_i using Freeman's algorithm⁵³ and then decompose it into fitting segments named $S_{i,k}$ (see Figure 5). Each segment $S_{i,k}$ has the properties, directrix $a_{i,k}$ and intercept $b_{i,k}$.

Extraction of Fiber Points. The extraction of points from a fiber relies on a process of finding nearly parallel facet matches. The parallel aspect between two facets of void boundaries related to the same fiber is rarely detected. We have therefore developed a procedure (Algorithm 1) to allow the matching of facets showing a certain degree of parallel aspect between them. The procedure and the algorithm are described below.

Let $P1$ be a void contour point designating a facet (Figure 6a or 6e). In the first step, we detect the parallel aspect, following a tolerance between two facets represented by $P1$ and $P2$ (Figure 6b or 6f). In the second step, we construct the parallel line of $P1$ passing through $P2$ that we call $D1'$ (Figure 6c or 6g) and then the point $P1'$ resulting from the intersection between the orthogonal line $D1'$ passing through $P1$ (Figure 6d or 6f). If the latter is connected to the boundary of an empty space, then the portion $(P1, P1')$ constitutes a fiber cut.

According to the method presented above and after the operations performed by Algorithm 1, we extract in EF the fiber portions (Figure 8). The set of points named $PSO_{i,k,j,l}$

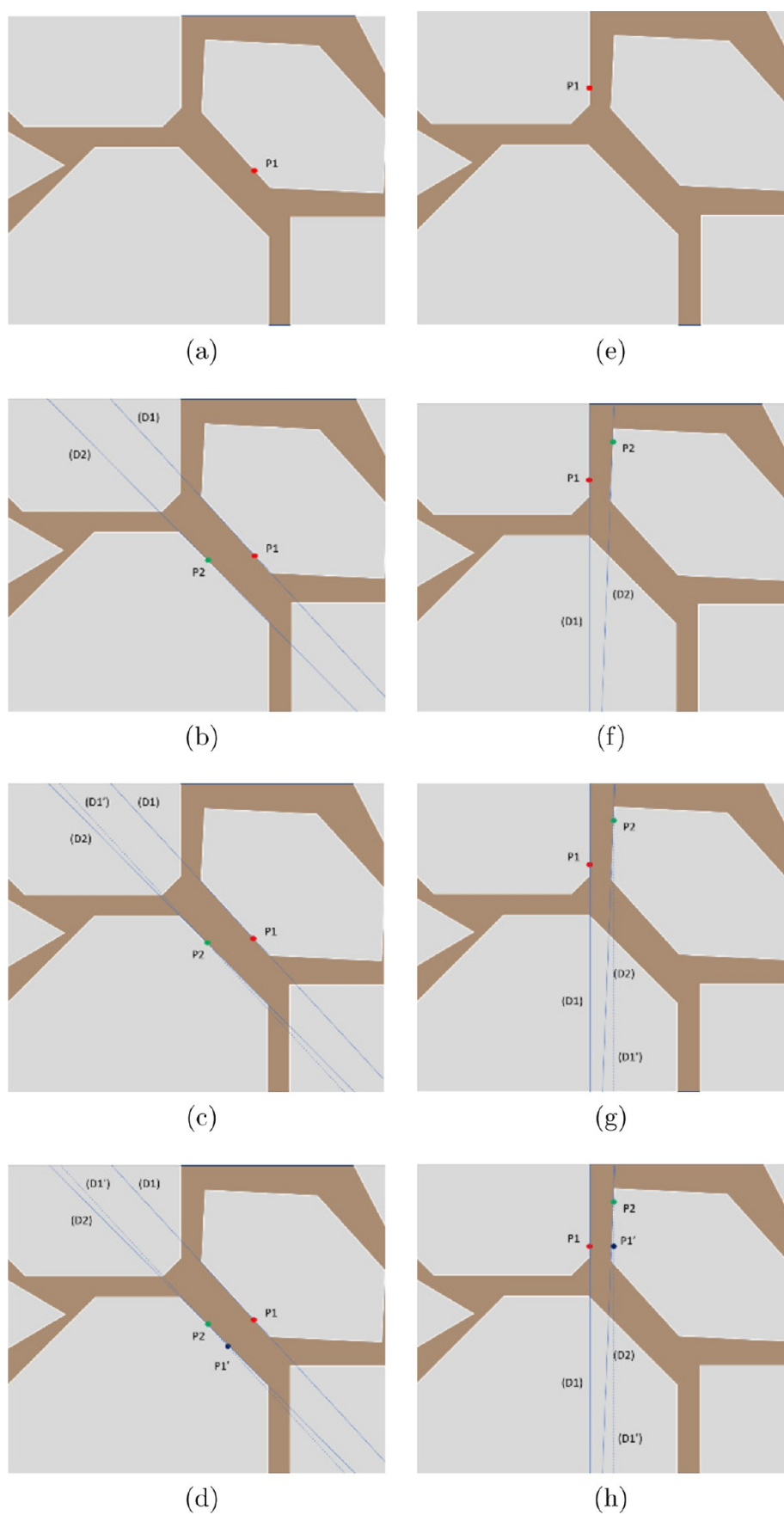


Figure 6. Illustration of the nearly parallel facet-matching process. (a–d) Extraction of a fiber portion that passed the parallel aspect test; (e–h) extraction that failed.

Algorithm 1 Extraction of points designating fiber portions.

```

1: for each segment  $S_{i,k}$  of  $T_i$  do
2:   for each segment  $S_{j,l}$  of  $T_j$  do
3:     if  $(i \neq j)$  and  $\exists$  segment  $SO_{i,k,j,l}$  orthogonal to  $S_{i,k}$  in  $P1_{(x,y)}$  and orthogonal to  $S_{j,l}$ 
       in  $P2_{(x,y)}$  and  $P1_{(x,y)} \in C$  and  $P2_{(x,y)} \in C$  and  $\forall P_{(x,y)} \in SO_{i,k,j,l} \Rightarrow P1_{(x,y)} \in EF$  and
        $SO_{i,k,j,l} \cap EV = \emptyset$  then
4:       Construct  $PSO_{i,k,j,l}$  center of  $SO_{i,k,j,l}$ 
5:     end if
6:   end for
7: end for

```

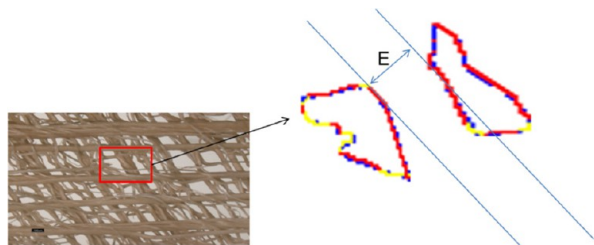


Figure 7. Extraction of fiber portions. On the left, fiber sample; on the right, the representation of an extracted fiber portion. In blue are designated the contours of a void area. In red are represented chains of mini segments of similar directions. In yellow are represented sequences of mini segments whose directions are not similar. E is the spacing between two nearly parallel edges.

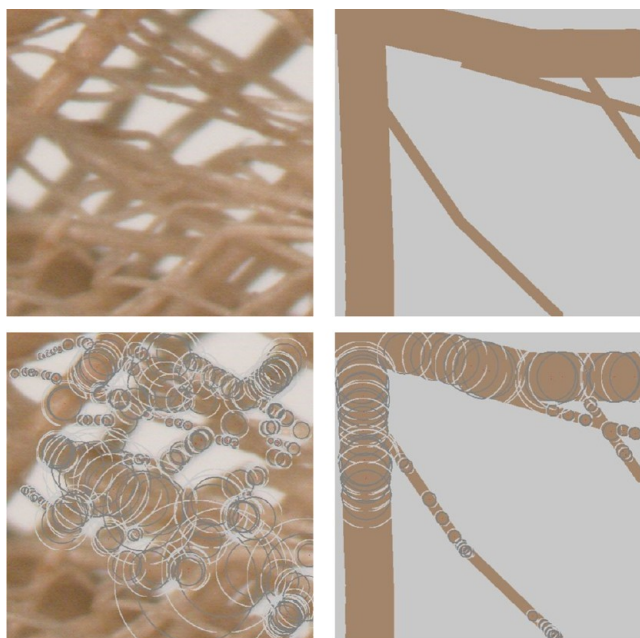


Figure 8. Results from Algorithm 1 on simulated data on the left and real data on the right. Circles indicate the portions extracted from the fiber.

constitutes a first extraction of points of interest designating fiber portions. Each of these points is provided with the property direction (Figure 7, blue lines) and thickness of the fiber (Figure 7, E). These starting points, which constitute initialization elements, will allow the construction of the entirety of the fibers.

Figure 8 shows the results obtained on simulated and real data.

Result of the proposed Algorithm 1 is a set of initial points whose position and thickness are known. These data constitute portions of coconut palm leaf sheath fibers that can be used to completely reconstruct the fibers they designate.

Search for Additional Points Designating the Fibers.

The first processing phase (section) highlighted portions of coconut palm leaf sheath fiber by exploiting the boundaries of void spaces, so as to extract areas of parallel aspects between the walls of a fiber. In the second phase of extraction, we use the points obtained after the application of Algorithm 1. These serve as initialization data for Algorithm 2, whose objective is the extraction of additional points designating a fiber. We group these initial points according to their membership in each of the fibers they represent, in order to construct the fibers I_{ij} , such that $I_{ij} = PSO_{i,k,j,l}(k,l) \in N \times N$. Thus, to construct EF (Algorithm 2) from near, we search from I_{ij} for new points $PSO_{i,k,j,l}$ (Figure 9). These points are provided with the thickness and direction features from the properties of I_{ij} .

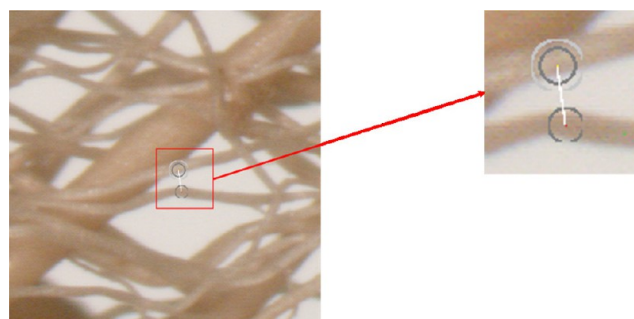


Figure 9. Extraction of additional points designating a fiber. The red point, belonging to the fiber in treatment, is used as a starting point to search for a new point (yellow), which is subjected to all the criteria to be able to integrate the fiber in reconstruction.

Algorithm stops when no more new points meeting the criteria of the fiber are discovered in the reconstruction phase. The final result is a set of new points assigned to one of the sets I_{ij} and belonging to EF designating a fiber of the image (Figure 10).

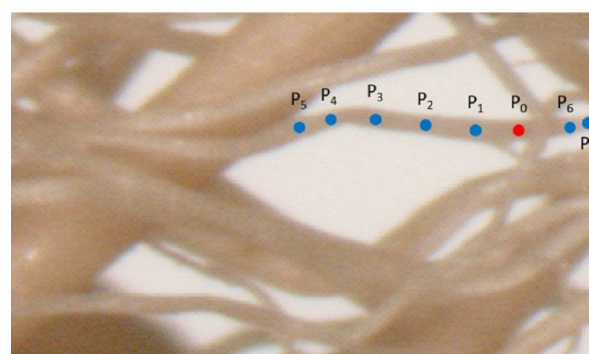


Figure 10. Extraction of additional points designating a fiber. The red point, belonging to the fiber in treatment, is used as a starting point to determine the new points (blue) that have verified all the criteria to integrate the fiber in reconstruction.

EXPERIMENTAL SECTION

Generation of Simulated Data. First, we simulated several data sets in order to evaluate the algorithms implemented in this work. Then, according to parameters such as number, thickness, and orientation angle, the fibers considered as thick as well as thin were detected. Thus, for these fibers, we have their location and all their properties. To

Algorithm 2 Extraction of additional points designating a fiber.

```

1: for each set of  $I_{i,j}$  do
2:    $m0 := -1$ 
3:    $m1 := 0$ 
4:   while ( $m0! = m1$ ) do
5:     if  $\exists B(P_{(x,y)}, thickness) \subset EF$  and  $[PSO_{i,k,j,l}, P_{(x,y)}] \subset EF$  and  $B(P_{(x,y)}, thickness) \cap F_i \neq \emptyset$  and  $angle(direction, [PSO_{i,k,j,l}, P_{(x,y)}]) \leq 90$  and  $d(P_{(x,y)}, PSO_{i,k,j,l}) \leq m1$  then
6:        $m0 := m1$ 
7:        $m1 := d(P_{(x,y)}, PSO_{i,k,j,l})$ 
8:       add  $P_{(x,y)}$  to the set of  $I_{i,j}$ 
9:     end if
10:  end while
11: end for

```

measure the effectiveness of the methods, we look at two criteria in particular. The first one concerns the possibility to detect and represent the maximum number of fibers correctly; it is estimated by comparing the pixels of the data set used to those provided as a result by the proposed algorithm. The second one checks for the detected fibers, whether the thickness and angle values are identical to those of the simulated data. These two procedures allow us to evaluate the relevance and quality of the algorithm. Let H and W be the dimensions chosen to represent a leaf sheath fiber area. We have a map called Simulation, which represents the simulated fibers for which we know, for each generated fiber, the positions, the directions, and the thicknesses. We introduce the sequences (NFE) and (NFF) as well as couples $(x1, y1)$ and $(x2, y2)$ as parameters of Algorithm 3, with NFE, the number of thick fibers; NFF, the number of thin fibers; and $(x1, y1)$ and $(x2, y2)$, coordinates of the points materializing the fiber under construction.

The values 90 and 175 represent the maximum angles that a thin and thick fiber twist can undergo, respectively.

Algorithm 3 Generate simulated data.

```

Require:  $mapresult := 0$ 
1: for INFE 1 to NFE do
2:    $xm := -1$ 
3:    $ym := -1$ 
4:   if  $random(0, 1) = 0$  then
5:      $x1 := 0$ 
6:      $y1 := random(0, H)$ 
7:   else
8:      $x1 := random(0, W)$ 
9:      $y1 := 0$ 
10:  end if
11:  while  $x1 \geq 0$  and  $x1 \leq W$  and  $y1 \geq 0$  and  $y1 \leq H$  do
12:     $x2 := random(-1, W + 1)$ 
13:     $y2 := random(-1, H + 1)$ 
14:    while  $xm! = -1$  and  $ym! = -1$  and  $angle([(xm, ym); (x1, y1)], [(x1, y1); (x2, y2)]) < 175$  do
15:      draw and expand  $FE/2$  thickness the segment  $[(x1, y1); (x2, y2)]$  in  $mapresult$ 
16:       $xm := x1$ 
17:       $ym := y1$ 
18:       $x1 := x2$ 
19:       $y1 := y2$ 
20:    end while
21:  end while
22: end for
23: for INFF 1 to NFF do
24:    $xm := -1$ 
25:    $ym := -1$ 
26:   while  $mapresult(x1, y1) = 0$  do
27:      $x1 := random(0, W)$ 
28:      $y1 := random(0, H)$ 
29:   end while  $stopgenerationFF := 1$ 
30:   while  $x1 \geq 0$  and  $x1 \leq W$  and  $y1 \geq 0$  and  $y1 \leq H$  and  $stopgenerationFF = 1$  do
31:      $x2 := random(-1, W + 1)$ 
32:      $y2 := random(-1, H + 1)$ 
33:     while  $xm! = -1$  and  $ym! = -1$  and  $angle([(xm, ym); (x1, y1)], [(x1, y1); (x2, y2)]) < 90$  do
34:       draw and expand  $FF/2$  thickness the segment  $[(x1, y1); (x2, y2)]$  in  $mapresult$ 
35:        $xm := x1$ 
36:        $ym := y1$ 
37:        $x1 := x2$ 
38:        $y1 := y2$ 
39:     end while
40:   end while
41: end for

```

These parameters are the essential elements of the simulated data generation process illustrated in Figure 11.



Figure 11. Extraction of additional points designating a fiber. The red point, belonging to the fiber in treatment, is used as a starting point to determine the new points (blue) that have verified all the criteria to integrate the fiber in reconstruction.

Real Data Acquisition. The real data are obtained from images taken with a binocular magnifier. These high-resolution images are cut into thumbnails with a size that fully represents the walls of the large fibers. To perform the processing, we chose a square of dimensions 500×500 pixels. These thumbnails can overlap in order to correct border problems during the reconstruction of the initial image.

Some examples of real data are shown in Figure 12.

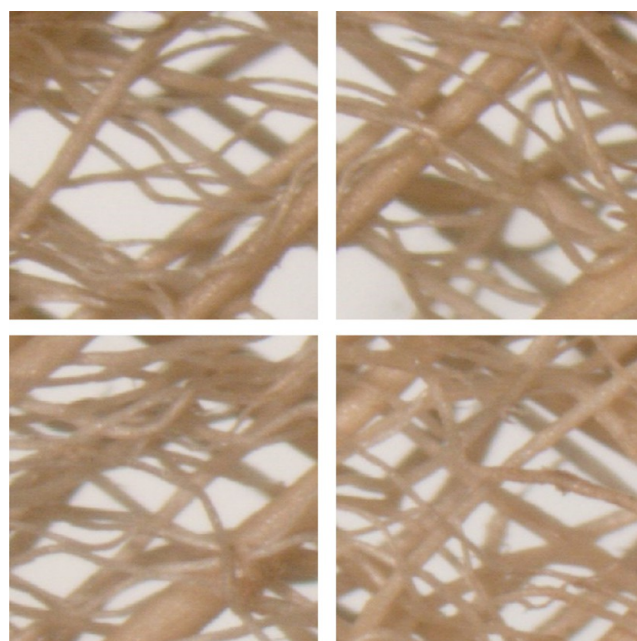


Figure 12. Examples of real data.

RESULTS AND DISCUSSION

Evaluation of the Spatial Representation of the Reconstructed Fibers. In order to evaluate the detection performance of the pixels designating the fiber, we use two criteria: sensitivity (3) and specificity (4).

$$\text{sensitivity} = \frac{\text{TP}}{\text{TP} + \text{FN}} \quad (3)$$

$$\text{specificity} = \frac{\text{TN}}{\text{TN} + \text{FP}} \quad (4)$$

with the following definitions: true positive, true negative, false positive, and false negative.

These parameters are calculated from the binary IR images (EF pixels are set to 1 and EV pixels are set to 0) produced by the reconstruction algorithms Eqs 5 and 6 and from the original reference images called IOR according to the instructions below.

$$\text{IOM}_{(x,y)} = \begin{cases} 1 & \text{if } P(x, y) \text{ is a fiber point} \\ 0 & \text{else} \end{cases} \quad (5)$$

$$\text{IR}_{(x,y)} = \begin{cases} 1 & \text{if } P(x, y) \text{ is calculated as a fiber point} \\ 0 & \text{else} \end{cases} \quad (6)$$

Initialize true positive (TP), true negative (TN), false positive (FP), and false negative (FN) to 0.

Compute for all image pixels,

if $\text{IOM}_{(x,y)} = 1$ and $\text{IR}_{(x,y)} = 1$, then increment TP,

if $\text{IOM}_{(x,y)} = 0$ and $\text{IR}_{(x,y)} = 0$, then increment TN,

if $\text{IOM}_{(x,y)} = 0$ and $\text{IR}_{(x,y)} = 1$, then increment FP,

if $\text{IOM}_{(x,y)} = 1$ and $\text{IR}_{(x,y)} = 0$, then increment FN.

The evolution of fiber generation Algorithm 3 on the number of thick fibers and the number of thin fibers, respectively, in the intervals [1; 4] and [1; 5] chosen in our study displays the results shown in Table 1.

The application of the process on the simulated data that resulted in the graph in Figures 13 and 17 shows an illustration of the results of the reconstructions performed by the algorithms implemented on the simulated data.

The sensitivity remains above 80% despite the increase in the number of fibers. The evolution of this parameter indicates that the developed methods correctly detect the points designating a fiber. In a similar way, the specificity, which oscillates around 80%, allows us to draw the same conclusion on the localization of points belonging to empty areas. These performances attest that the algorithms implemented meet the problem of spatial reconstruction of fibers.

The results of the evaluation of the fiber reconstruction analysis, on real data represented by about 100 thumbnails, are shown in Table 2.

The scores on real data are on average above 50%. We observe a rate of 62% for sensitivity, which reveals a correct detection of the points designating a fiber. The 73% rate for specificity attests that the points identified by our procedures really belong to empty areas. The more pronounced results in the case of simulated data are justified by the fact that we do not take into account alterations in the walls of the fibers, which are then less smooth. After analysis of this report, it appears that for the algorithms developed within the framework of the study, the schematization of an open mesh of leaf sheath is more representative of reality compared to a

Table 1. Sensitivity and Specificity Parameter Values on the Number of Thick Fibers and the Number of Thin Fibers, in the Respective Intervals [1; 4] and [1; 5]

(thick fibers; fine fibers)	sensitivity	specificity	accuracy
(1; 0)	0.99	0.78	0.95
(1; 1)	0.99	0.79	0.96
(1; 2)	0.99	0.87	0.97
(1; 3)	0.99	0.89	0.96
(1; 4)	0.97	0.88	0.95
(1; 5)	0.99	0.85	0.95
(2; 0)	0.99	0.83	0.94
(2; 1)	0.98	0.77	0.92
(2; 2)	0.97	0.77	0.92
(2; 3)	0.97	0.90	0.95
(2; 4)	0.98	0.46	0.85
(2; 5)	0.92	0.90	0.1
(3; 0)	0.95	0.89	0.92
(3; 1)	0.95	0.89	0.92
(3; 2)	0.97	0.86	0.93
(3; 3)	0.96	0.75	0.88
(3; 4)	0.95	0.82	0.89
(3; 5)	0.95	0.83	0.90
(4; 0)	0.94	0.91	0.93
(4; 1)	0.97	0.86	0.92
(4; 2)	0.95	0.76	0.86
(4; 3)	0.97	0.79	0.89
7(4; 4)	0.94	0.61	0.75
(4; 5)	0.91	0.86	0.88

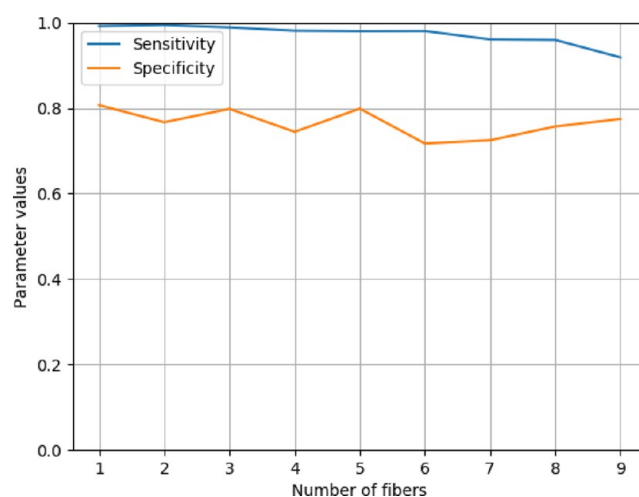


Figure 13. Evolution of sensitivity and specificity parameters on simulated data.

dense mesh. Indeed, in the case of very dense meshes, they represent them in important proportion by empty spaces.

This result corroborates 170 human observations, designating the problem areas for the algorithms as those comprising the tight fiber clusters.

Evaluation of the Characterization of the Reconstructed Fibers. In evaluating the characterization of the reconstructed fibers, we pay particular attention to the quality of the thickness and direction attributes extracted by our algorithms. Table 3 presents the reproduction rates of the simulated points. These rates are a function of the mapping between a simulated point and a reconstructed point. The result is considered relevant if a simultaneous match is

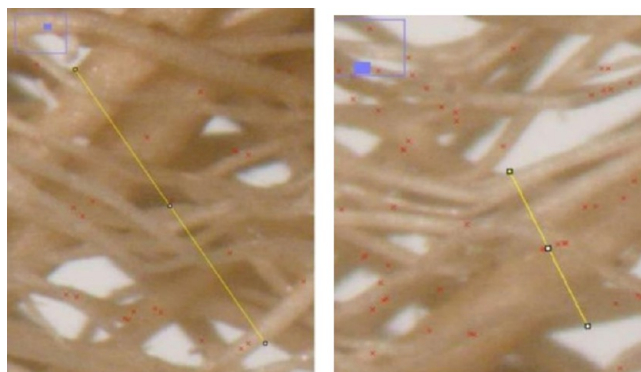


Figure 14. Portions of fibers abnormally detected by the algorithms. The yellow cut segments represent the thickness of the automatically detected fiber portions, actually forming a cluster.

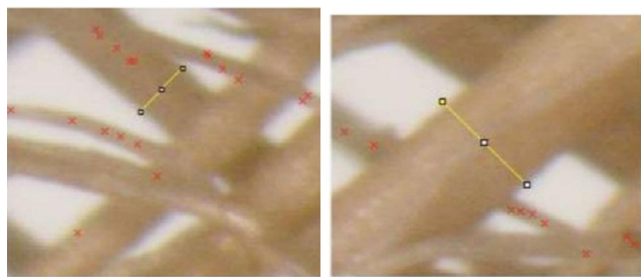


Figure 15. Fiber portions correctly detected by the algorithms. The cut segments in yellow represent the thickness of the automatically detected fiber portions. Construction of a model from the data generated by the implemented algorithms.

obtained between the position of the points and the thickness and direction attributes assigned to these points.

During the automatic evaluation process between the simulated and reconstructed attributes, we first performed a spatial match between the points and then compared the thicknesses and orientation angles. The results obtained for this study show that the values are globally above 50% success rate. However, there is a slight difference between the points matched in space. The rates obtained on the thicknesses as well as the orientation angles show that it is still necessary to refine the reconstruction of these attributes, which are, respectively, at 59.86% and 61.76% of correspondence, measured without correlation between the two. The total correspondence between all the criteria—position, thickness, and orientation angle—is around 58.51% on the 17,345 simulated points.

Estimation of the actual values with Image J software, as part of the algorithm validity study, revealed that clusters of tightly packed fibers with no voids between the fibers are considered and evaluated by the application as a single fiber. Two examples related to this case are shown in Figure 14.

As a consequence of the previous situation, we decided to evaluate with the Image J software only the thicknesses and the orientation angles, with respect to the horizontal, of the spaced fibers that the model detects as unit fibers (Figure 15).

For these fibers, Student's *t*-test allows us to conclude, with a risk of 5%, that the values predicted by the algorithms and those measured with the Image J software do not present a significant difference, and this for the two morphological characteristics evaluated (thickness and angle) (Figure 16).

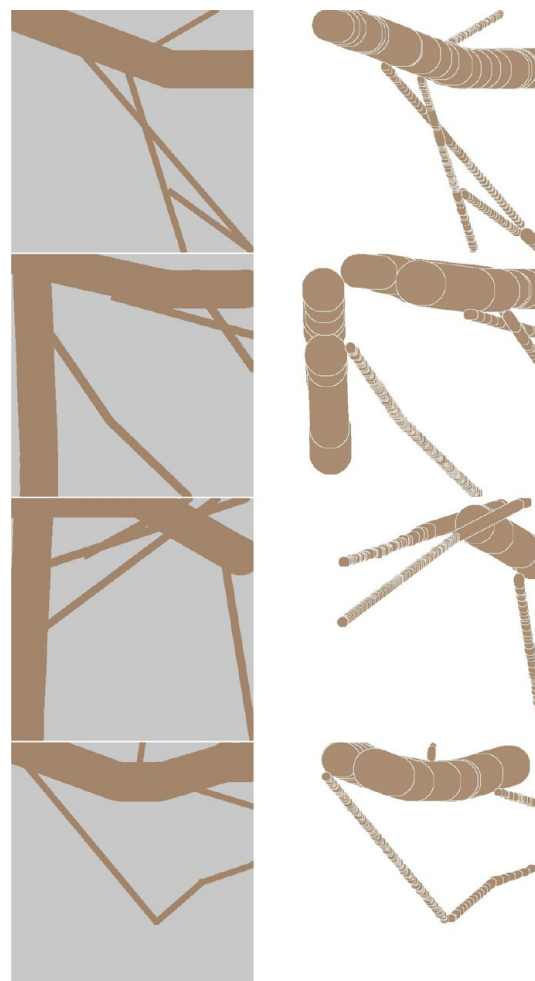


Figure 16. Illustration of the reconstruction capabilities of the models implemented on simulated data. On the left column are the simulated fiber images and on the right their reconstructions by the implemented algorithms.

On the data generated by the implemented algorithms, we construct two operators. These operators will be used to increase the number of points constructed from the data generated by Algorithms 1 and 2. Let N be the maximum number of fibers extracted from the fiber image support; for any $n \in [1; N]$ we have

$$f_0(n) = (x, y) \text{ tq } B\left((x, y), \frac{\text{thickness}}{2}\right) \cap \text{EF} \neq \emptyset \quad (7)$$

where (x, y) is a point in EF and thickness is the thickness of the fiber.

The second operator is established as follows:

$$\forall (x, y) \text{ of } f_0 \text{ then } f(x, y) = (\text{angle}, \text{thickness}, n)$$

where angle is the angle formed by the fiber and the horizontal direction.

These two expressions offer the possibility of exploiting methods from the literature such as the study of textures or the study of frequencies of appearance of patterns in the sites of high extraction rate. The areas with low extraction rates can be better reconstructed using extrapolation from the use of these new operators. Some examples of reconstructions of coir fiber portion from the mathematical models derived from the results of the implemented algorithms are shown in Figures 13 and 17.

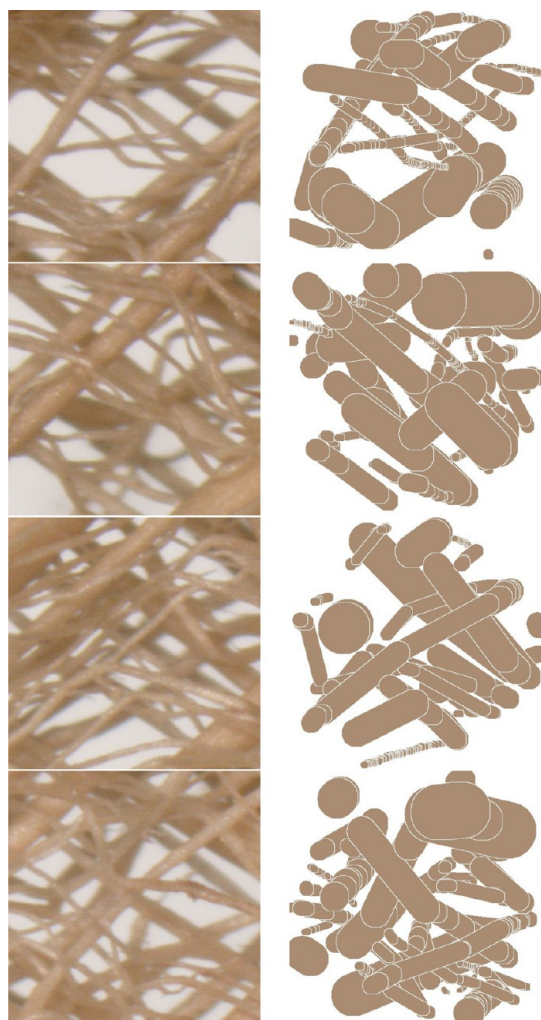


Figure 17. Illustration of the reconstruction capabilities of the models implemented on real data. On the left column are the fiber images and on the right their reconstructions by the implemented algorithms.

Table 2. Treatment Results with Sensitivity and Specificity Parameters on Real Data

operator	sensitivity	specificity
Average	0.628097557	0.735190848
Standard deviation	0.1362069	0.062656945

Table 3. Reconstruction Rate of the Algorithms on the Simulated Data

simulated points	number of matches			
	position (%)	thickness (%)	angle (%)	total (%)
17345	65.53	59.86	61.76	58.51

CONCLUSIONS

The characterization of coconut palm leaf sheath fibers, mostly the study of fiber organization, is an important issue in the perspective of realizing future materials more respectful of our environment based on vegetable materials. The integration of natural fibers in the design of new materials aims to make human achievements more ecological. In this context, we proposed during this work two algorithms allowing from digital images of fibers and the extraction of attributes. The first algorithm that we proposed uses the aspect of the empty zones

in the mesh of the leaf sheath, to match nearly parallel walls in order to constitute initial portions of fibers. The second algorithm allows us to reconstruct from the extracted portions the entirety of the unitary fibers present in the processed image. We then extract from these treatments three primitives: position, orientation, and thickness, characterizing a unit fiber in the mesh of the leaf sheath. The evaluations carried out on simulated data as well as on real data using the sensitivity and specificity criteria showed the effectiveness of the treatments implemented. The data obtained can then be used to assist experts in their knowledge extraction and characterization of the leaf sheath of *C. nucifera* L. (2D).

PERSPECTIVES

In the future work, we envisage a complementary contribution by allowing the learning and the automatic recognition of redundant structures, by introducing a learning network of tensors flow type, with the objective of implementing attributes in input of the system. Moreover, the mathematical model that will be implemented will provide the network with the properties of the areas where the fibers could not be extracted. We also plan to use a more efficient color segmentation method better adapted to the optical microscope. We believe that the development of new processes is necessary to determine as many shapes as possible in the images and to perform a finer extraction in the less contrasted areas.

AUTHOR INFORMATION

Corresponding Author

Jimmy Nagau – LAMIA Laboratory, 97157 Pointe-a-Pitre, Guadeloupe; Department of Mathematic Computer Science, Université des Antilles, 97157 Pointe-à-Pitre Cedex, Guadeloupe, France; orcid.org/0000-0002-4225-0433; Phone: +590 690 737679; Email: jimmy.nagau@univ-antilles.fr

Authors

Lisa Vidil – COVACHIM-M2E Laboratory, 97157 Pointe-a-Pitre, Guadeloupe; Department of Chemistry, Université des Antilles, 97157 Pointe-à-Pitre Cedex, Guadeloupe, France

Cristel Onesippe Potiron – COVACHIM-M2E Laboratory, 97157 Pointe-a-Pitre, Guadeloupe; Department of Chemistry, Université des Antilles, 97157 Pointe-à-Pitre Cedex, Guadeloupe, France

Ketty Bilba – COVACHIM-M2E Laboratory, 97157 Pointe-a-Pitre, Guadeloupe; Department of Chemistry, Université des Antilles, 97157 Pointe-à-Pitre Cedex, Guadeloupe, France

Marie-Ange Arsene – COVACHIM-M2E Laboratory, 97157 Pointe-a-Pitre, Guadeloupe; Department of Chemistry, Université des Antilles, 97157 Pointe-à-Pitre Cedex, Guadeloupe, France

Jean-Luc Henry – LAMIA Laboratory, 97157 Pointe-a-Pitre, Guadeloupe; Department of Mathematic Computer Science, Université des Antilles, 97157 Pointe-à-Pitre Cedex, Guadeloupe, France

Complete contact information is available at: <https://pubs.acs.org/10.1021/acsomega.2c02748>

Notes

The authors declare no competing financial interest.

REFERENCES

- (1) Onésippe, C. La biomasse biosourcée pour l'élaboration et la caractérisation de matériaux: des complexes pour parois de microcapsules aux composites pour l'habitat et la construction, French Post-doctoral degree. Ph.D. Thesis, Université des Antilles, 2020.
- (2) Arsène, M.-A. Elaboration et caractérisation de matériaux: cas de semi-conducteurs et de matériaux issus de sous-produits lignocellulosiques tropicaux, French Post-doctoral degree. Ph.D. Thesis, Université des Antilles et de la Guyane, 2006.
- (3) Bilba, K. Elaboration et caractérisation de matériaux composites, French Post-doctoral degree. Ph.D. Thesis, Université des Antilles et de la Guyane, 2006.
- (4) Harle, S. M. The performance of natural fiber reinforced polymer composites. *Int. J. Civ. Eng. Res.* **2014**, *5*, 285–288.
- (5) Lau, K.-t.; Hung, P.-y.; Zhu, M.-H.; Hui, D. Properties of natural fibre composites for structural engineering applications. *Compos. B Eng.* **2018**, *136*, 222–233.
- (6) Cristaldi, G.; Latteri, A.; Recca, G.; Cicala, G. Composites based on natural fibre fabrics. *Woven Fabr. Eng.* **2010**, *17*, 317–342.
- (7) Rajesh, M.; Sultan, M. T. H.; Uthayakumar, M.; Jayakrishna, K.; Shah, A. U. M. Dynamic behaviour of woven bio fiber composite. *Bioresources* **2018**, *13*, 1951–1960.
- (8) Fidelis, M. E. A.; Pereira, T. V. C.; Gomes, O. d. F. M.; de Andrade Silva, F.; Toledo Filho, R. D. The effect of fiber morphology on the tensile strength of natural fibers. *J. Mater. Res. Technol.* **2013**, *2*, 149–157.
- (9) Tran, L. Q. N.; Minh, T. N.; Fuentes, C.; Chi, T. T.; Van Vuure, A. W.; Verpoest, I. Investigation of microstructure and tensile properties of porous natural coir fibre for use in composite materials. *Ind. Crops Prod.* **2015**, *65*, 437–445.
- (10) Stolyarov, O.; Ershov, S. Experimental study and finite element analysis of mechanical behavior of plain weave fabric during deformation through a cross-section observation. *Mater. Today Commun.* **2022**, *31*, 103367.
- (11) Fiore, V.; Scalici, T.; Valenza, A. Characterization of a new natural fiber from Arundo donax L. as potential reinforcement of polymer composites. *Carbohydr. Polym.* **2014**, *106*, 77–83.
- (12) Martin, N.; Davies, P.; Baley, C. Comparison of the properties of scutched flax and flax tow for composite material reinforcement. *Ind. Crops Prod.* **2014**, *61*, 284–292.
- (13) Azanaw, A.; Haile, A.; Gideon, R. K. Extraction and characterization of fibers from Yucca Elephantine plant. *Cellulose* **2019**, *26*, 795–804.
- (14) Ibrahim, M.; Moustafa, H.; Rahman, E. N. A. E.; Mehanny, S.; Hemida, M. H.; El-Kashif, E. Reinforcement of starch based biodegradable composite using Nile rose residues. *J. Mater. Res. Technol.* **2020**, *9*, 6160–6171.
- (15) Venkateshappa, S. C.; Bennehalli, B.; Kenchappa, M. G.; Ranganagowda, R. P. G. Flexural behaviour of areca fibers composites. *Bioresources* **2010**, *5*, 1846–1858.
- (16) Orue, A.; Jauregi, A.; Unsuaín, U.; Labidi, J.; Eceiza, A.; Arbelaz, A. The effect of alkaline and silane treatments on mechanical properties and breakage of sisal fibers and poly (lactic acid)/sisal fiber composites. *Compos. Appl. Sci. Manuf.* **2016**, *84*, 186–195.
- (17) Zhang, X. Manufacturing of hemp/PP composites and study of its residual stress and aging behavior. Ph.D. Thesis, Université de Technologie de Troyes, 2016.
- (18) Shibata, M.; Takachiyo, K.-I.; Ozawa, K.; Yosomiya, R.; Takeishi, H. Biodegradable polyester composites reinforced with short abaca fiber. *J. Appl. Polym. Sci.* **2002**, *85*, 129–138.
- (19) Bavan, D. S.; Kumar, G. M. Potential use of natural fiber composite materials in India. *J. Reinf. Plast. Compos.* **2010**, *29*, 3600–3613.
- (20) Fadele, O.; Oguocha, I. N.; Odeshi, A.; Soleimani, M.; Karunakaran, C. Characterization of raffia palm fiber for use in polymer composites. *J. Wood Sci.* **2018**, *64*, 650–663.
- (21) Bezazi, A.; Belaadi, A.; Bourchak, M.; Scarpa, F.; Boba, K. Novel extraction techniques, chemical and mechanical characterisation of Agave americana L. natural fibres. *Compos. B Eng.* **2014**, *66*, 194–203.
- (22) Hossain, M. R.; Islam, M. A.; Van Vuure, A.; Verpoest, I. Quantitative analysis of hollow lumen in jute. *Procedia Eng.* **2014**, *90*, 52–57.
- (23) Abdennadher, A. Injection Moulding of Natural Fibre Reinforced Polypropylene: Process, Microstructure and Properties. Ph.D. Thesis, Ecole Nationale Supérieure des Mines de Paris, 2015.
- (24) Maache, M.; Bezazi, A.; Amroune, S.; Scarpa, F.; Dufresne, A. Characterization of a novel natural cellulosic fiber from Juncus effusus L. *Carbohydr. Polym.* **2017**, *171*, 163–172.
- (25) Garat, W.; Corn, S.; Le Moigne, N.; Beaugrand, J.; Bergeret, A. Analysis of the morphometric variations in natural fibres by automated laser scanning: towards an efficient and reliable assessment of the cross-sectional area. *Compos. Appl. Sci. Manuf.* **2018**, *108*, 114–123.
- (26) Vidil-Ratiarisoa, L. Etude de matériaux naturels 2D : Potentialités d'utilisation comme renfort de matériaux composites. Ph.D. Thesis, Université des Antilles, 2019.
- (27) Amel, B. A.; Paridah, M. T.; Sudin, R.; Anwar, U.; Hussein, A. S. Effect of fiber extraction methods on some properties of kenaf bast fiber. *Ind. Crops Prod.* **2013**, *46*, 117–123.
- (28) Ticoalu, A.; Aravinthan, T.; Cardona, F. A study into the characteristics of gomuti (Arenga pinnata) fibre for usage as natural fibre composites. *J. Reinf. Plast. Compos.* **2014**, *33*, 179–192.
- (29) Bachtiar, E. V.; Kurkowiak, K.; Yan, L.; Kasal, B.; Kolb, T. Thermal stability, fire performance, and mechanical properties of natural fibre fabric-reinforced polymer composites with different fire retardants. *Polymers* **2019**, *11*, 699.
- (30) Jeyanthi, S.; Rani, J. J. Development of natural long fiber thermoplastic composites for automotive frontal beams. *Indian J. Eng. Mater. Sci.* **2014**, *21*, 580–584.
- (31) Sunny, T.; Pickering, K. L.; Lim, S. H. Alignment of short fibres: an overview. *Process. Fabr. Adv. Mater.* **2017**, 616–625.
- (32) Misnon, M. I.; Islam, M. M.; Epaarachchi, J. A.; Lau, K.-t. Potentiality of utilising natural textile materials for engineering composites applications. *Mater. Des.* **2014**, *59*, 359–368.
- (33) Li, Y.; Sreekala, M.; Jacob, M. *Textile composites based on natural fibers*; Old City Publishing, 2009.
- (34) Karaduman, N. S.; Karaduman, Y.; Ozdemir, H.; Ozdemir, G. Textile reinforced structural composites for advanced applications. *Text. Adv. Appl.* **2017**, *87*. DOI: 10.5772/intechopen.68245
- (35) Baran, I.; Cinar, K.; Ersoy, N.; Akkerman, R.; Hattel, J. H. A review on the mechanical modeling of composite manufacturing processes. *Arch. Comput. Methods Eng.* **2017**, *24*, 365–395.
- (36) Pham, M. Q.; Döbrich, O.; Trümper, W.; Gereke, T.; Cherif, C. Numerical modelling of the mechanical behaviour of biaxial weft-knitted fabrics on different length scales. *Materials* **2019**, *12*, 3693.
- (37) Brown, L. P.; Zeng, X.; Long, A.; Jones, I. A., et al. Recent developments in the realistic geometric modelling of textile structures using TexGen. *Proceedings of the 1st international conference on digital technologies for the textile industries*; University of Nottingham, 2013; p 6.
- (38) Vilfayeu, J.; Crépin, D.; Boussu, F.; Soulat, D.; Boisse, P. Kinematic modelling of the weaving process applied to 2D fabric. *J. Ind. Textil* **2015**, *45*, 338–351.
- (39) Dixit, A.; Mali, H. S. Modeling techniques for predicting the mechanical properties of woven-fabric textile composites: a review. *Mech. Compos. Mater.* **2013**, *49*, 1–20.
- (40) Zeng, X.; Brown, L. P.; Endruweit, A.; Matveev, M.; Long, A. C. Geometrical modelling of 3D woven reinforcements for polymer composites: Prediction of fabric permeability and composite mechanical properties. *Compos. Appl. Sci. Manuf.* **2014**, *56*, 150–160.
- (41) Lomov, S. V.; Huysmans, G.; Luo, Y.; Parnas, R.; Prodromou, A.; Verpoest, I.; Phelan, F. Textile composites: modelling strategies. *Compos. Appl. Sci. Manuf.* **2001**, *32*, 1379–1394.
- (42) Lomov, S. V.; Verpoest, I. Modelling of the internal structure and deformability of textile reinforcements: WiseTex software.

Proceeding of 10th European Conf. Composite Materials (ECCM-10), Brugge, Belgium; Katholieke Universiteit Leuven, 2002; pp 3–7.

(43) Lomov, S. V.; Willems, A.; Verpoest, I.; Zhu, Y.; Barburski, M.; Stoilova, T. Picture frame test of woven composite reinforcements with a full-field strain registration. *Text. Res. J.* **2006**, *76*, 243–252.

(44) Verpoest, I.; Lomov, S. V. Virtual textile composites software WiseTex: Integration with micro-mechanical, permeability and structural analysis. *Compos. Sci. Technol.* **2005**, *65*, 2563–2574.

(45) Couégnat, G. *Approche multiéchelle du comportement mécanique de matériaux composites à renfort tissé*. Ph.D. Thesis, Université Sciences et Technologies-Bordeaux I, 2008.

(46) Sherburn, M. *Geometric and mechanical modelling of textiles*. Ph.D. Thesis, University of Nottingham Nottingham, 2007.

(47) Afrashteh, S.; Merati, A. A.; Jeddi, A. A. A. *Geometrical parameters of yarn cross-section in plain woven fabric*; NISCAIR-CSIR, 2013.

(48) Hivet, G.; Boisse, P. Consistent 3D geometrical model of fabric elementary cell. Application to a meshing preprocessor for 3D finite element analysis. *Finite Elem. Anal. Des.* **2005**, *42*, 25–49.

(49) Hivet, G.; Boisse, P. Consistent mesoscopic mechanical behaviour model for woven composite reinforcements in biaxial tension. *Compos. B Eng.* **2008**, *39*, 345–361.

(50) Wendling, A.; Hivet, G.; Vidal-Sallé, E.; Boisse, P. Consistent geometrical modelling of interlock fabrics. *Finite Elem. Anal. Des.* **2014**, *90*, 93–105.

(51) Wendling, A.; Daniel, J.; Hivet, G.; Vidal-Sallé, E.; Boisse, P. Meshing preprocessor for the Mesoscopic 3D finite element simulation of 2D and interlock fabric deformation. *Appl. Compos. Mater.* **2015**, *22*, 869–886.

(52) Bourmaud, A.; Beaugrand, J.; Shah, D. U.; Placet, V.; Baley, C. Towards the design of high-performance plant fibre composites. *Prog. Mater. Sci.* **2018**, *97*, 347–408.

(53) Freeman, H. Computer processing of line-drawing images. *ACM Comput. Surv.* **1974**, *6*, 57–97.